Chapter 1
Sensitivity-Based Substructure Error Propagation for Efficient Assembly Model Reduction

B. M. Kessels, M. L. J. Verhees, A. M. Steenhoek, R. H. B. Fey, and N. van de Wouw

Abstract Due to ever-increasing complexity of structural dynamic systems in various fields of engineering, model reduction techniques using a substructuring approach, a.k.a. component mode synthesis techniques, still form an active field of research. This paper proposes an efficient, novel method for error approximation for model reduction of coupled substructures in structural dynamics. When coupling multiple reduced substructure models, the influence of individual substructure modes on the dynamic behavior of the total reduced mechanical assembly is generally unknown. Rather than selecting substructure eigenmodes, which are used to constitute the reduction bases, solely based on their eigenfrequencies, this paper proposes a different selection method. This method inspects the influence of individual substructure modes on an assembly receptance using so-called modal receptance error contributions. These modal receptance error contributions are defined as the assembly receptance reduction error induced by truncating individual substructure modes. By determining the sensitivity of the receptance of the assembly with respect to the uncoupled substructure receptances, a substructure reduction error is propagated through the assembly model, resulting in a first-order approximation of the assembly error. To calculate this sensitivity, the receptance of the assembly is expressed in terms of the individual receptances of the uncoupled substructures and Boolean mapping matrices, used to couple substructures. Comparing different modal receptance error contributions, associated with the reduction of individual substructures, provides insight in the selection of substructure modes which results in an efficient reduction of the assembly. As such, a mode-selection criterion is defined by using the obtained information on the sensitivity of the quality of the assembly reduction to truncating individual substructure modes. This criterion helps to determine a more efficient reduction basis. To illustrate the proposed method, a cantilever Euler beam consisting of two substructures is used.

Keywords Structural dynamics · Model reduction · CMS · Substructure mode selection · Error Propagation

1.1 Introduction

Modeling structural dynamics systems continues to be a challenging task due to the ever-increasing complexity of these systems. Furthermore, despite the advances in computer technology, this growing complexity makes computational work increasingly time consuming. One of the many fields where these problems are relevant is the semiconductor industry. For instance, lithographic systems, required for semiconductor production, demand extreme levels of accuracy and consequently detailed and accurate models. The finite element models required to achieve this accuracy generally have too many Degrees Of Freedom (DOFs) to be used within reasonable computational time. Therefore, the development of methodologies which reduce the size and complexity of these numerical models, while maintaining a desired level of accuracy, is still an active research field. A disadvantage of decreasing the number of DOFs is the resulting loss of the accuracy of the reduced model, which can be quantified by the difference between the responses and/or dynamic properties of the reduced model and similar

B. M. Kessels (✉) · R. H. B. Fey · N. van de Wouw
Eindhoven University of Technology, Department of Mechanical Engineering, Eindhoven, The Netherlands

University of Minnesota, Department of Civil, Environmental, and Geo-Engineering, Minneapolis, MN, USA
e-mail: b.m.kessels@tue.nl; r.h.b.fey@tue.nl; n.v.d.wouw@tue.nl

M. L. J. Verhees · A. M. Steenhoek
ASML, System Dynamics, Veldhoven, The Netherlands
e-mail: thijs.verhees@asml.com; alexander.steenhoek@asml.com

M. S. Allen et al. (eds.), *Dynamic Substructures, Volume 4*, Conference Proceedings of the Society for Experimental Mechanics Series, https://doi.org/10.1007/978-3-030-75910-0_1

quantities of the unreduced model. Therefore, reduction methods have been devised which try to optimize the trade-off between improvement of the efficiency and loss of accuracy.

An example of such reduction methods is moment matching [1]. Since this method is applied in the frequency domain, useful insights as would be obtained in the time domain (e.g., eigenvalues with corresponding mode shapes of reduced structures) are lost though. Two other well-established reduction methods are balanced truncation [1] and Hankel norm approximation [8], which both focus on maintaining accurate input–output behavior. Although both methods provide useful a priori bounds on the reduction error, the first-order description of the system used for these methods loses physical interpretability after reduction. A fourth class of reduction methods which does not suffer from loss of physical insight are Component Mode Synthesis (CMS) methods [2], in which components are reduced by truncating component vibration modes, targeting on accuracy in a certain range of frequencies.

To manage the complexity of models, they are often divided into multiple substructures or components which can be modeled and analyzed separately. This approach is referred to as Dynamic Substructuring (DS) [10]. Additionally, the number of DOFs of each substructure model can be decreased to reduce computational costs. Subsequently, the reduced substructure models are coupled to obtain a reduced assembly model. The methods belonging to the aforementioned class of CMS methods use the concept of DS. Often, static (correction) modes are involved in the process of coupling substructure models, i.e., realizing compatibility of neighboring interface DOFs and achieving internal interface force equilibrium. Therefore, these static modes are typically present in the reduction bases of CMS methods. Additionally, typically, a selection of other mode-types, e.g., retained (or non-truncated) eigenmodes, is present in these reduction bases as well. Depending on the specific CMS method, the types of employed eigenmodes vary. For example, the Craig–Bampton method [3] uses eigenmodes of a substructure which is virtually constrained at its interfaces with other substructures. Oppositely, the Hintz–Herting (HH) method [9], for instance, uses eigenmodes which are free at the interfaces.

The truncation of eigenmodes is usually done by selecting eigenmodes based on their eigenfrequencies. Since high-frequency behavior is typically of less interest than the behavior at low frequencies, eigenmodes with low eigenfrequencies are usually retained, whereas high-frequency eigenmodes are truncated [7, 9, 10]. Although this approach is often viable, the set of "kept" eigenmodes might not be optimal when multiple substructures are coupled. This statement is motivated by the fact that some (local) component eigenmodes, or even entire substructures, may have very little influence on the behavior of (relevant) assembly transfer functions. Hence, low-frequency component eigenmodes, which have only little influence on the relevant assembly behavior, are unnecessarily retained, leaving room for improvement. In addition, high-frequency component eigenmodes that show relevant (local) behavior might be truncated. Techniques that evaluate the influence of component modes on the assembly transfer function in order to select which modes should be retained are however scarce. More specifically, techniques that select component modes such that specific error measures of reduced assembly transfer functions are minimized seem to be missing in literature. Therefore, this paper proposes a novel method which, based on a sensitivity analysis, selects substructure eigenmodes resulting in an accurate and efficient reduction basis for each component. As will be shown, this method yields reduced assembly models with lower reduction errors compared to assembly models which are reduced using the traditional component eigenmode-selection method, i.e., using eigenfrequencies. Since the method presented here requires free-interface eigenmodes, the previously mentioned Hintz–Herting CMS method is adopted for this research.

The proposed method is based on the propagation of substructure errors which is efficiently approximated by exploiting a sensitivity-based description of the assembly reduction receptance error as explained in Sect. 1.2. This section also discusses an approximation of the substructure receptance error which improves the efficiency of the selection procedure. Subsequently, Sect. 1.3 explains how the estimated assembly receptance error is used to select substructure eigenmodes. Results obtained for a case study, where a beam system consisting of two substructures is used, are then presented in Sect. 1.4. Finally, the conclusions and some suggestions for future work are listed in Sect. 1.5.

1.2 Sensitivity-Based Substructure Error Propagation

In this section, an efficient approach to estimate the error in the assembly receptance originating from substructure reduction errors is introduced. To achieve this, the assembly receptance error is described in terms of individual contributions of substructure receptance errors using a first-order approximation [5]:

$$\boldsymbol{\Delta Y}^{(assy)}(j\omega) = \sum_{k}^{n_{uc}} \sum_{l}^{n_{uc}} \frac{\partial \boldsymbol{Y}^{(assy)}}{\partial \boldsymbol{Y}[k,l]}(\omega j)\, \boldsymbol{\Delta Y}^{(uc)}[k,l](j\omega). \tag{1.1}$$

Here, matrix $\boldsymbol{\Delta Y}^{(assy)}$ denotes the approximated error in the assembly receptance matrix $\boldsymbol{Y}^{(assy)}$, n_{uc} denotes the combined number of all DOFs of all uncoupled components, and ω denotes the angular eigenfrequency. This error consists of the product of two multiplication factors: (i) the sensitivity of the assembly with respect to a change in a single component $(\frac{\partial \boldsymbol{Y}^{(assy)}}{\partial \boldsymbol{Y}[k,l]})$, and (ii) the receptance error induced in the uncoupled components $(\boldsymbol{\Delta Y}^{(uc)}[k,l])$, where $\boldsymbol{\Delta Y}^{(uc)}$ contains the uncoupled component receptance error matrices $\boldsymbol{\Delta Y}^{(s)}$ on its diagonal, and $[k,l]$ selects the matrix-element in row k and column l. These terms are derived separately in the following exposition, starting with the former.

1.2.1 Sensitivity of Assembly with Respect to a Substructure

The first multiplication factor in the right-hand side of (1.1) serves to separate the contributions of individual substructures to the assembly error. To isolate these contributions, the Lagrange Multiplier Frequency-Based Substructuring (LM FBS) framework is adopted [6]. This framework defines the assembly receptance matrix as

$$\boldsymbol{Y}^{(assy)} = \boldsymbol{Y} - \boldsymbol{Y}\boldsymbol{Q}\boldsymbol{Y}, \tag{1.2}$$

where

$$\boldsymbol{Q} = \boldsymbol{B}_f^T \left(\boldsymbol{B}_f \boldsymbol{Y} \boldsymbol{B}_f^T\right)^{-1} \boldsymbol{B}_f. \tag{1.3}$$

Here, $\boldsymbol{Y}$ is a block diagonal matrix containing the uncoupled substructure receptance matrices in the blocks on its diagonal and $\boldsymbol{B}_f$ is a signed Boolean mapping matrix ensuring compatibility at the substructure interfaces. Exploiting the linearity of a matrix with respect to its elements, the partial derivative of (1.2) with respect to $\boldsymbol{Y}[k,l]$ is efficiently calculated:

$$\frac{\partial \boldsymbol{Y}^{(assy)}}{\partial \boldsymbol{Y}[k,l]} = \boldsymbol{P}_{kl} - \boldsymbol{P}_{kl}\boldsymbol{Q}\boldsymbol{Y} + \boldsymbol{Y}\boldsymbol{Q}\boldsymbol{P}_{kl}\boldsymbol{Q}\boldsymbol{Y} - \boldsymbol{Y}\boldsymbol{Q}\boldsymbol{P}_{kl}, \tag{1.4}$$

where $\boldsymbol{P}_{kl}$ is a single-entry matrix with $\boldsymbol{P}_{kl}[k,l] = 1$. For a detailed derivation of (1.4), the reader is referred to [4].

1.2.2 Error in Uncoupled Substructures

The second multiplication factor in the right-hand side of (1.1) is the (estimated) reduction receptance error within a substructure. Since these reduced substructures are to be coupled, CMS is used for the reduction [10]. Although (1.1) contains multiple substructure receptance error matrices contained in a block diagonal matrix $(\boldsymbol{\Delta Y}^{(uc)})$, this section focuses on the computation of a single reduction receptance error matrix of substructure s $(\boldsymbol{\Delta Y}^{(s)})$, where the explicit dependency on s is omitted for clarity in the following. One method to achieve this reduction is the aforementioned Hintz–Herting CMS method [9], in which the reduction matrix is defined as

$$\boldsymbol{T}_{HH} = \left[\boldsymbol{\Phi}_{\mathcal{K}}\ \boldsymbol{\Phi}_{\mathrm{ir}}\ \boldsymbol{\Psi}_{\mathrm{const}}\right] =: \left[\boldsymbol{\Phi}_{\mathcal{K}}\ \boldsymbol{X}\right]. \tag{1.5}$$

Here, $\boldsymbol{\Phi}_{\mathrm{ir}}$ represents a set containing n_{ir} inertia relief modes and $\boldsymbol{\Psi}_{\mathrm{const}}$ is a set consisting of n_b constraint modes which ensure statically exact behavior at the boundary nodes [9]. The set of boundary nodes is constituted by the nodes at the interfaces and nodes at which external forces/moments are applied. Furthermore, $\boldsymbol{\Phi}_{\mathcal{K}}$ represents a set of $n_{\mathcal{K}} \leq n_{DOF} - n_{ir} - n_b$ kept free-interface eigenmodes, where n_{DOF} represents the number of DOFs in the substructure. Although typically the eigenmodes with the lowest associated eigenfrequencies are used to constitute this set, other combinations of (kept) eigenmodes can be used as well. Note that in (1.5), in contrast to the definition found in [9], $\boldsymbol{\Phi}_{\mathrm{ir}}$ and $\boldsymbol{\Psi}_{\mathrm{const}}$ are orthogonalized with respect to $\boldsymbol{\Phi}_{\mathcal{K}}$. This orthogonality ensures that the reduced mass, stiffness, and, when modal damping is assumed, damping matrices are of a block diagonal nature. Consequently, a (partial) spectral decomposition of the HH reduced receptance matrix of a substructure is acquired:

$$\begin{aligned}\hat{\boldsymbol{Y}}_{HH}(j\omega) &= \boldsymbol{Y}_{\boldsymbol{X}}(j\omega) + \sum_{k\in\mathcal{K}} \boldsymbol{Y}_{\boldsymbol{\phi}_k}(j\omega)\\ &=: \boldsymbol{Y}_{\boldsymbol{X}}(j\omega) + \hat{\boldsymbol{Y}}_{\mathcal{K}}(j\omega),\end{aligned} \tag{1.6}$$

where $\mathcal{K}$ represents the set of mode numbers related to the set of kept modes. Furthermore, the receptance contribution of the inertia relief and constraint modes is defined as

$$\boldsymbol{Y}_{\boldsymbol{X}}(j\omega) = \boldsymbol{X}\left(\hat{\boldsymbol{K}}_X + j\omega\hat{\boldsymbol{D}}_X - \omega^2\hat{\boldsymbol{M}}_X\right)^{-1}\boldsymbol{X}^T, \tag{1.7}$$

which, if $n_{ir} + n_b$ is small, uses a relatively inexpensive inverse, and where

$$\hat{\boldsymbol{M}}_X = \boldsymbol{X}^T\boldsymbol{M}\boldsymbol{X}, \qquad \hat{\boldsymbol{D}}_X = \boldsymbol{X}^T\boldsymbol{D}\boldsymbol{X}, \qquad \hat{\boldsymbol{K}}_X = \boldsymbol{X}^T\boldsymbol{K}\boldsymbol{X}. \tag{1.8}$$

Alternatively, superposition of modal contributions to $\boldsymbol{Y}_X$ based on an eigenvalue problem constituted by $\hat{\boldsymbol{M}}_X$, $\hat{\boldsymbol{D}}_X$, and $\hat{\boldsymbol{K}}_X$ could be employed to calculate $\boldsymbol{Y}_{\boldsymbol{X}}$. Furthermore, in case of mass-normalized eigenmodes, the modal substructure receptance contributions in (1.6) are given by

$$\boldsymbol{Y}_{\boldsymbol{\phi}_k}(j\omega) = \frac{\boldsymbol{\phi}_k{\boldsymbol{\phi}_k}^T}{{\omega_k}^2 - 2j\xi_k\omega_k\omega - \omega^2}. \tag{1.9}$$

Note that, if $n_{\mathcal{K}} = n_{\text{DOF}} - n_{\text{ir}} - n_{\text{b}}$, the system is not reduced and thus the receptance matrix $\hat{\boldsymbol{Y}}_{HH}$ does actually not represent a reduced receptance and is therefore equivalent to the unreduced receptance matrix. Since the aim of the method proposed in this paper is to select which eigenmodes in the set $\mathcal{K}$ should be retained such that an accurate reduced assembly receptance is obtained, the influence of each eigenmode should be investigated. This is achieved by evaluating, for each eigenmode, what the receptance error would be if exclusively that eigenmode is truncated from the set $\mathcal{K}$, such that a set $\mathcal{K}_{\text{eval}}$ containing $n_{\mathcal{K}} - 1$ eigenmodes is obtained. In a practical setting, it is however often not feasible to compute all eigenmodes of a large system. The set $\mathcal{K}$ may therefore denote a limited set of eigenmodes obtained by a coarse modal truncation, in which a relatively large set of eigenmodes with the lowest eigenfrequencies are retained. In this case, the proposed eigenmode-selection method will select a subset of this large set $\mathcal{K}$ to form the new smaller set $\mathcal{K}_{\text{sel}}$ containing $n_{\text{sel}} < n_{\mathcal{K}}$ eigenmodes.

To avoid calculating $\boldsymbol{Y}_{\boldsymbol{X}}(j\omega)$, which depends on the specific set of kept modes, for each evaluated set $\mathcal{K}_{\text{eval}}$ such that the corresponding HH receptance reduction error is obtained, the Modal Truncation (MT) receptance error is used instead. This error is computed relatively cheaply for multiple small sets of individually truncated eigenmodes using modal superposition:

$$\boldsymbol{\Delta Y} = \sum_{k\in\mathcal{D}_{\text{eval}}} \boldsymbol{Y}_{\boldsymbol{\phi}_k}(j\omega) = \sum_{k\in\mathcal{D}_{\text{eval}}} \frac{\boldsymbol{\phi}_k{\boldsymbol{\phi}_k}^T}{{\omega_k}^2 - 2j\xi_k\omega_k\omega - \omega^2}. \tag{1.10}$$

Here, $\boldsymbol{\phi}_k$, ω_k, and ξ_k denote the kth eigenmode, kth angular eigenfrequency, and kth modal damping factor, respectively. Furthermore, $\mathcal{D}_{\text{eval}}$ represents the set of deleted (or truncated) eigenmodes, which in the proposed methodology thus contains only a single eigenmode for each evaluation. Note that, as shown in (1.6), the HH reduced receptance ($\hat{\boldsymbol{Y}}_{HH}$) is not exactly equal to the MT reduced receptance ($\hat{\boldsymbol{Y}}_{\mathcal{K}}$) due to the influence of $\boldsymbol{Y}_{\boldsymbol{X}}(j\omega)$. Nevertheless, it is expected that an "optimal" selection of eigenmodes $\mathcal{K}_{\text{sel}}$, obtained using an analysis based on the MT receptance error, is a valid approximation of the "optimal" set of eigenmodes for a HH reduction basis. This is motivated by the fact that the addition of $\boldsymbol{Y}_{\boldsymbol{X}}(j\omega)$ in (1.6) always improves the accuracy of $\hat{\boldsymbol{Y}}_{\mathcal{K}}$. Therefore, in order to achieve an "optimal" $\hat{\boldsymbol{Y}}_{HH}$, it is assumed that it is best practice to first find the "optimal" $\hat{\boldsymbol{Y}}_{\mathcal{K}}$. Accordingly, (1.10) is substituted, together with (1.4), in (1.1) to estimate the assembly receptance reduction error caused by truncating a single substructure eigenmode. A methodology which uses this approximation to determine which sets of substructure eigenmodes constitute substructure MT reduction bases that minimize the assembly receptance error is introduced in the following section. The sets of eigenmodes found using this methodology are then used in combination with the constraint and inertia relief modes in HH reduction bases to reduce the substructures which are eventually coupled to obtain the reduced assembly model.

1.3 Component Mode Selection

In this section, the approximated assembly receptance reduction error is used to directly assess the influence of individual substructure eigenmodes on the assembly receptance reduction error. For this assessment, a leave-one-out approach is adopted where the (additional) assembly receptance error, caused by truncation of a single eigenmode, is estimated for each substructure eigenmode and in all substructures. Although the error of each assembly Frequency Response Function (FRF) related to all DOFs in the receptance matrix can be taken into account, often only a limited number of assembly FRFs, related to the n_{POIs} Points Of Interest (POIs), is relevant. Here, the latter approach will be adopted. Consequently, the estimated receptance reduction error of these relevant FRFs are stored in a (square) matrix $\boldsymbol{\Delta Y}^{(assy)}_{\text{POIs}}$. This receptance error matrix is a function of the frequency. Therefore, first, spatial norms of the assembly receptance error matrix are calculated at each evaluated frequency point, resulting in a vector where each entry corresponds to a single frequency point. Subsequently, a "temporal" norm is used such that this vector is condensed to a single scalar error quantity. These scalar values (obtained by truncating different substructure eigenmodes) make comparing errors significantly more straightforward and suitable for automation. The procedure of taking spatial and temporal norms is schematically summarized in Fig. 1.1.

In this work, the Frobenius norm is used as spatial norm since it takes the value of each matrix-entry into account with equal weight (note that a separate weighting matrix can however be added if required):

$$\hat{\epsilon}^{(assy)}(\omega) = \frac{\left\| \boldsymbol{\Delta Y}^{(assy)}_{\text{POIs}}(j\omega) \right\|_F}{\left\| \boldsymbol{Y}^{(assy)}_{\text{POIs}}(j\omega) \right\|_F}. \tag{1.11}$$

Here, the hat on top of ϵ represents the approximated nature of this (frequency-dependent) error measure. Additionally, as shown in (1.11), the Frobenius norm of the receptance error is divided by the Frobenius norm of the unreduced receptance matrix such that a relative norm is obtained. This choice is motivated by the assumption that the response at all frequencies should be approximated equally well in a relative sense. A temporal norm, specifically the 2-norm, is then used to condense the frequency-dependent error measure $\hat{\epsilon}^{(assy)}(\omega)$ into a single scalar error quantity:

$$\hat{\chi}^{(assy)} = \left\| W(\omega)\hat{\epsilon}^{(assy)}(\omega) \right\|_2, \tag{1.12}$$

where $W(\omega)$ represents a frequency-filtering function. In this paper, brick-wall filtering is used to exclusively evaluate errors within a specified Frequency Range Of Interest (FROI).

As mentioned before, a leave-one-out approach is adopted to establish the set of kept substructure eigenmodes. For each free-interface eigenmode k of each substructure s, the error measure $\hat{\chi}^{(assy)}_{\boldsymbol{\phi}^{(s)}_k}$ is calculated as if mode k of component s would be the only mode to be truncated in the entire assembly. Afterwards, all error measures of all substructures are sorted by magnitude. The eigenmodes related to the $n^{(assy)}_{\mathcal{K}}$ highest error measures are then selected as (kept) vibration modes in the new (HH) reduction bases of each substructure. Here, $n^{(assy)}_{\mathcal{K}}$ can be chosen a priori by the user based on required model sizes (in terms of, e.g., number of DOFs). Alternatively, the choice of $n^{(assy)}_{\mathcal{K}}$ can be based on a required (maximal) error level.

Finally, note that the set of eigenmodes, found using (estimated) receptance errors, will be equivalent to the set of eigenmodes that is found based on (estimated) mobility and inertance errors. This statement is using the fact that a time derivative in the frequency domain is a multiplication with $j\omega$ which is negated by the relative norm in (1.11).

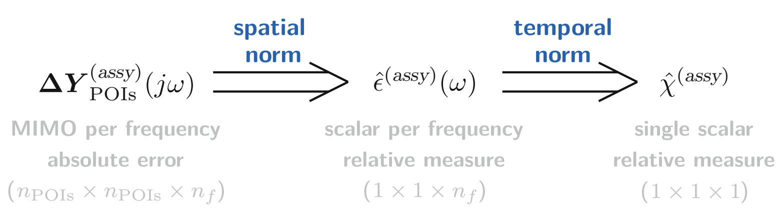

Fig. 1.1 Schematic overview of the procedure to determine the relative error measure by using spatial and temporal norms. Indicated between brackets are the dimensions of each variable/measure (n_{POIs} is the number of POIs and n_f is the number of evaluated frequency points)

1.4 Results

1.4.1 Demonstrator Description

To illustrate the method introduced in the previous sections, a simple Euler–Bernoulli cantilever beam is used. As shown in Fig. 1.2, this beam is cut in half to obtain two substructures. The material and geometry parameters of both substructures are listed in Table 1.1 (note the relatively low Young's modulus for substructure A). Additionally, proportional modal damping is added to each free-interface eigenmode of both substructures with $\xi = 0.05$ for all eigenmodes. To model the substructures, they are divided into 10 identical linear 2-node Euler beam elements each, resulting in 11 nodes per substructure, where each node has one transversial displacement and one rotational DOF. Consequently, the unreduced models of components A and B have 20 and 22 DOFs, respectively, and the unreduced assembly model has 40 DOFs. As indicated in Fig. 1.2, one node per substructure is required for coupling and is labeled as interface node. These interface nodes are part of the set of boundary nodes. Other nodes belonging to the set of boundary nodes are the nodes at which external forces/moments are applied. These nodes are also referred to as retained nodes. Since these boundary nodes represent relevant nodes in the system, they are also referred to as points of interest. In this example, only the transfer functions between the forces and moments, and displacements and rotations at the POIs are considered relevant. Therefore, $\boldsymbol{Y}^{(assy)}_{\mathrm{POIs}}$ and $\boldsymbol{\Delta Y}^{(assy)}_{\mathrm{POIs}}$ exclusively contain the FRFs related to DOFs of the boundary nodes.

1.4.2 Ranking of Substructure Eigenmodes

As discussed earlier, the first step in the mode-selection procedure is to estimate the assembly errors caused by truncating individual modes, $\boldsymbol{\Delta Y}^{(assy)}_{\boldsymbol{\phi}^{(s)}_k}$, using (1.1). Then, the estimated error measures $\hat{\chi}^{(assy)}_{\boldsymbol{\phi}^{(s)}_k}$ are obtained by first applying (1.11) to $\boldsymbol{\Delta Y}^{(assy)}_{\boldsymbol{\phi}^{(s)}_k}$ and then using (1.12). Both the frequency-dependent error measures based on the spatial norm, i.e., $\hat{\epsilon}^{(assy)}(\omega)$, and the scalar error measures, i.e., $\hat{\chi}^{(assy)}$, are plotted in Fig. 1.3 for the first two free-interface eigenmodes of both substructures. As illustrated by this figure, the error measures for the eigenmodes of substructure A are clearly higher than those of substructure B. Note that there is a large difference in $\hat{\epsilon}^{(assy)}$ at low frequencies. Therefore, these eigenmodes of substructure A should be kept in the reduced model of substructure A, since they are expected to cause relatively large errors, if truncated, compared to the examined eigenmodes of substructure B.

In Table 1.2, the scalar error measures related to all (elastic free-interface) eigenmodes of both substructures, obtained for a FROI $= 0 - 32$ Hz, are listed. This table also specifies the eigenfrequency of each eigenmode. Note that, due to the use of the MT receptance error approximation as introduced in Section II, there is no limitation on the number of evaluated

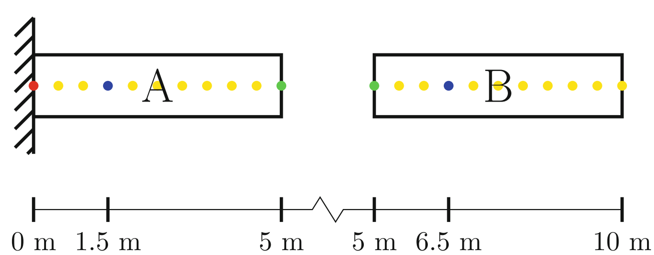

Fig. 1.2 Schematic representation of a two-substructure cantilever beam. The fixed, interface, retained, and internal nodes of each substructure are indicated by the red, green, blue, and yellow dots, respectively

Table 1.1 Material and geometry parameters for the two-substructure cantilever beam

Parameter	Unit	Substructure A	Substructure B
Density	kg/m^3	7.850×10^3	7.850×10^3
Cross-sectional area	m^2	1×10^{-2}	1×10^{-2}
Area moment of inertia	m^4	$1/12 \times 10^{-4}$	$1/12 \times 10^{-4}$
Young's modulus	N/m^2	2.1×10^9	2.1×10^{11}

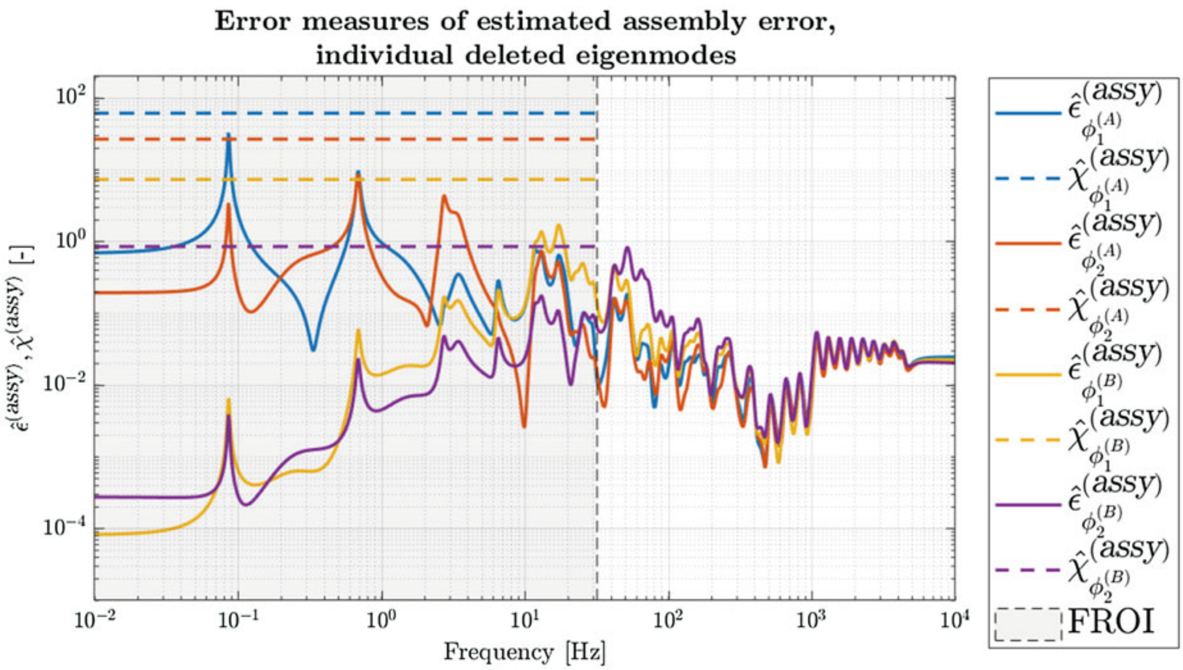

Fig. 1.3 Approximated assembly receptance error measures $\hat{\epsilon}^{(assy)}(\omega)$ and $\hat{\chi}^{(assy)}$, obtained by deleting specific substructure free-interface eigenmodes, with FROI $= 0 - 32$ Hz

Table 1.2 Eigenfrequencies and estimated scalar error measures for the assembly receptance error when only a single substructure elastic free-interface eigenmode is truncated, listed for every eigenmode of both substructures of the demonstrator beam. The kth eigenfrequency of unreduced substructure s is denoted by $f_k^{(s)}$

	Substructure A		Substructure B			Substructure A		Substructure B	
Mode k	$f_k^{(A)}$ [Hz]	$\hat{\chi}^{(assy)}_{\boldsymbol{\phi}_k^{(A)}}$ [−]	$f_k^{(B)}$ [Hz]	$\hat{\chi}^{(assy)}_{\boldsymbol{\phi}_k^{(B)}}$ [−]	Mode k	$f_k^{(A)}$ [Hz]	$\hat{\chi}^{(assy)}_{\boldsymbol{\phi}_k^{(A)}}$ [−]	$f_k^{(B)}$ [Hz]	$\hat{\chi}^{(assy)}_{\boldsymbol{\phi}_k^{(B)}}$ [−]
1	0.334	61.790	21.267	7.358	11	114.735	2.389	1372.920	0.036
2	2.095	26.832	58.636	0.854	12	138.614	1.413	1657.922	0.023
3	5.866	9.149	115.028	0.405	13	168.032	0.681	1992.830	0.028
4	11.503	8.964	190.428	0.238	14	202.804	1.353	2384.978	0.028
5	19.045	12.233	285.225	0.115	15	243.699	1.347	2843.043	0.018
6	28.532	3.188	400.022	0.081	16	291.466	1.022	3370.610	0.020
7	40.031	2.407	535.536	0.072	17	345.925	0.559	3949.969	0.024
8	53.631	4.835	691.699	0.046	18	403.850	1.030	4499.502	0.012
9	69.344	1.326	859.280	0.030	19	454.780	1.156	5686.193	0.058
10	86.205	0.713	1141.111	0.038	20	569.152	3.381	5696.749	0.057

eigenmodes due to concerns related to orthogonality of the HH reduction basis. Since for the demonstrator used here, all n_{DOF} eigenmodes can be calculated, each eigenmode of both substructures is evaluated. The error measures in Table 1.2 are sorted by magnitude, resulting in Table 1.3, where the 13 eigenmodes with the highest error measures are ranked (high to low) in the middle row. Additionally, the eigenmodes are ranked by eigenfrequency (low to high) in the last row as is done in the traditional eigenmode-selection procedure. As is shown in Table 1.3, some differences can be observed between the ranking of eigenmodes using the traditional method and using the newly proposed, or sensitivity-based, method. For example, according to the sensitivity-based method, the fifth eigenmode of substructure A is the third kept mode of choice, whereas it is the fifth mode of choice based on the eigenfrequencies. Also, the 8$^{\text{th}}$ eigenmode of substructure A is expected to be more relevant than modes 6 and 7 of substructure A according to the error measure-based ranking compared to the eigenfrequency-based ranking.

Now, using Table 1.3, substructure eigenmodes can be selected such that an accurate and efficient reduced assembly model is obtained. For the traditional method (using the cutoff frequencies of the component eigenmodes) the first $n_{\mathcal{K}}^{(assy)}$ eigenmodes in the "traditional method" row are selected, since these correspond to the eigenmodes with the lowest

Table 1.3 Ranking of the 13 most relevant elastic free-interface eigenmodes of both substructures, based on the newly proposed (sensitivity-based) and traditional (cutoff frequency) eigenmode-selection method. The error measures are determined for a FROI $= 0 - 32$ Hz

Ranking of substructure eigenmodes		1	2	3	4	5	6	7	8	9	10	11	12	13	…
Proposed method	Substructure	A	A	A	A	A	B	A	A	A	A	A	A	A	
	Mode	1	2	5	3	4	1	8	20	6	7	11	12	14	
Traditional method	Substructure	A	A	A	A	A	B	A	A	A	B	A	A	A	
	Mode	1	2	3	4	5	1	6	7	8	2	9	10	11	

eigenfrequencies. Oppositely, for the sensitivity-based method, the first $n_{\mathcal{K}}^{(assy)}$ eigenmodes in the "proposed method" row are selected, because these are expected to generate the highest assembly reduction error (measure) when truncated. Note that the different order of eigenmodes for both methods suggests that the traditional method is not optimal for the defined error measure.

In part C of this section, see below, three examples will be given in which the newly proposed selection method outperforms the traditional method. To compare both methods, the exact assembly receptance error will be used:

$$\boldsymbol{E}_{\text{POIs}}^{(assy)}(j\omega) = \boldsymbol{Y}_{\text{POIs}}^{(assy)}(j\omega) - \hat{\boldsymbol{Y}}_{\text{POIs}}^{(assy)}(j\omega). \tag{1.13}$$

In (1.13), $\hat{\boldsymbol{Y}}_{\text{POIs}}^{(assy)}$ is the reduced assembly receptance matrix obtained by reducing the substructures with a set of kept eigenmodes (as selected using Table 1.3), where only the FRFs corresponding to the POIs are contained within this matrix. To make this comparison fair and straightforward, similar error measures as used for the estimated receptance error measure calculation ((1.11) and (1.12)) are determined for the reduced assembly. Since now the assembly error is not estimated but exactly calculated for the sake of the comparison, the exact receptance error measures are denoted without hat, i.e., as $\epsilon^{(assy)}(\omega)$, and $\chi^{(assy)}$. To this end, the estimated assembly error, $\boldsymbol{\Delta Y}_{\text{POIs}}^{(assy)}$, in (1.11) is replaced by the exact assembly receptance error, $\boldsymbol{E}_{\text{POIs}}^{(assy)}$.

1.4.3 Comparison of Different Sets of Kept Eigenmodes

In this section, the exact assembly reduction errors as obtained by using the traditional and improved eigenmode-selection procedures are compared for 3 use cases.

In the first use case, it is assumed that the user only wants to retain 3 elastic free-interface eigenmodes for the Hintz–Herting reduction basis. Note that besides these eigenmodes, the required constraint and inertia relief modes are also present in the substructure reduction bases. Note that, in this example, the constraint modes of substructure B represent the rigid-body modes. Using the traditional selection method, solely elastic free-interface eigenmodes 1, 2, and 3 of substructure A would be kept in the reduction basis of substructure A, as indicated in Table 1.3. In contrast, the sensitivity-based method selects eigenmode 5 instead of 3 of substructure A. In Fig. 1.4, the associated exact receptance error measures of the resulting reduced assembly models are compared. As is shown in Fig. 1.4, $\epsilon^{(assy)}(\omega)$ indicates that the proposed method results in a favorable frequency-dependent error measure, especially near the end of the FROI. After taking the temporal norm, $\chi^{(assy)}$ is shown to be the lowest for the sensitivity-based method, as is also demonstrated in Table 1.5. This indicates that, in this case, with the same number of DOFs in the reduced model, the sensitivity-based selection method results in a more accurate reduced assembly receptance.

Since the first use case selects a relatively low amount of eigenmodes (note that the highest eigenfrequency of the 3 kept elastic free-interface eigenmodes is below the highest frequency in the FROI), for the second use case a larger set of eigenmodes is selected. More specifically, the number of eigenmodes is based on a rule of thumb often used in practice where the cutoff frequency used to reduce the substructures (by applying CMS) is approximately equal to 2.5 times the upper bound of the FROI. For the FROI investigated here, this implies that all eigenmodes with an eigenfrequency up to 80 Hz should be retained. Since, according to Table 1.2, there are in total 11 eigenmodes in both substructures with an eigenfrequency below 80 Hz, these eigenmodes are selected for the traditional approach. For a fair comparison in terms of computation time, the same number of eigenmodes is selected using Table 1.3 for the sensitivity-based method. As shown in Fig. 1.5, the sensitivity-based method results again in a lower receptance error measure, indicating that, also for this use case, the proposed

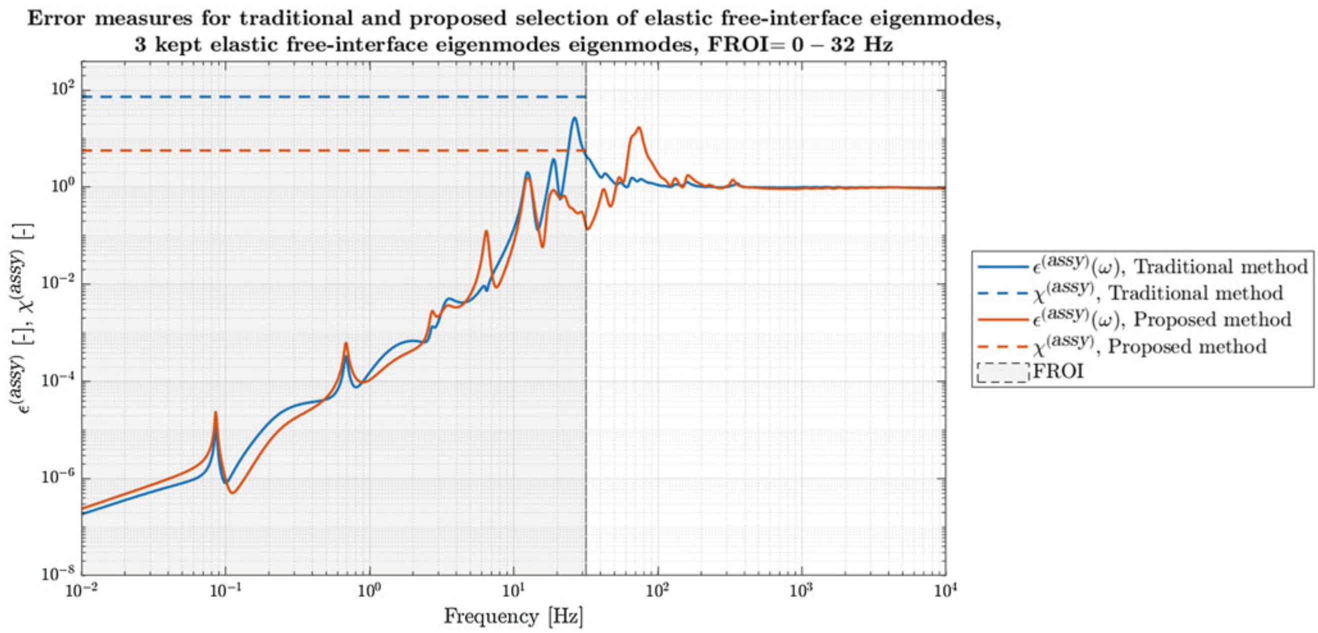

Fig. 1.4 Assembly receptance error measures $\epsilon^{(assy)}(\omega)$ and $\chi^{(assy)}$ obtained by using HH reduction bases where 3 elastic free-interface substructure eigenmodes are selected using the traditional method and the proposed method

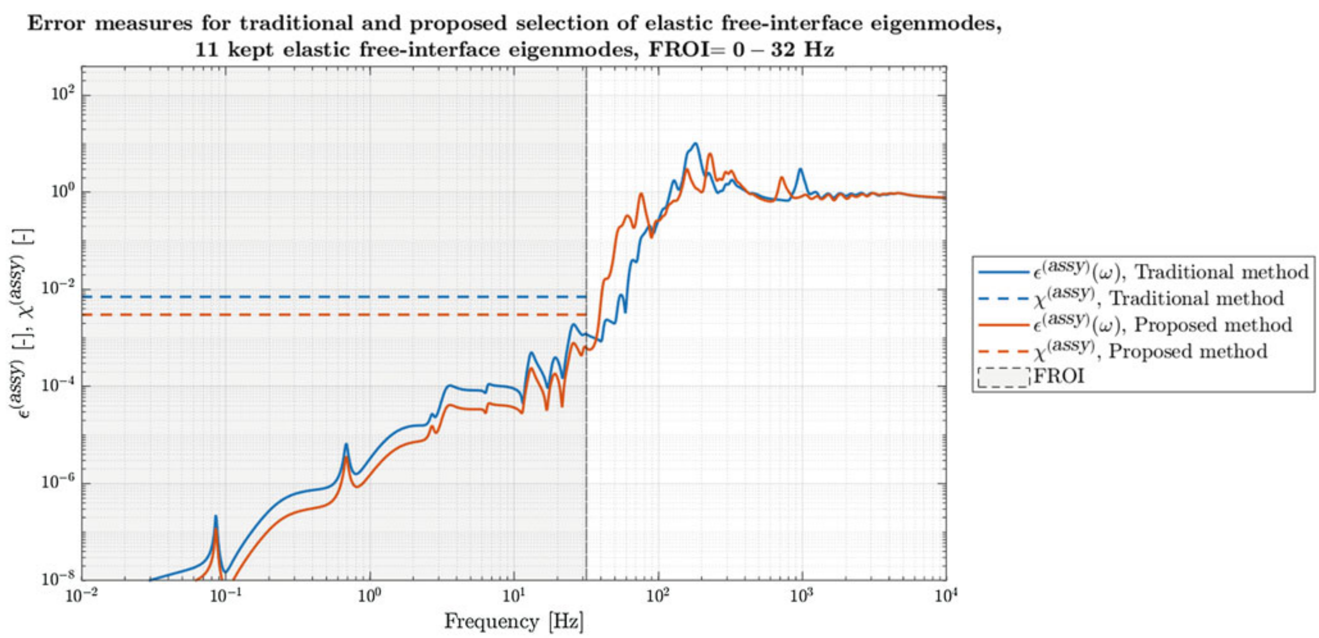

Fig. 1.5 Assembly receptance error measures $\epsilon^{(assy)}(\omega)$ and $\chi^{(assy)}$ obtained by using HH reduction bases where 11 elastic free-interface substructure eigenmodes are selected using the traditional method and the proposed method

method outperforms the traditional method. Furthermore, Fig. 1.5 also shows that the frequency-dependent receptance error measure of the sensitivity-based method is below that of the traditional method in the entire FROI.

Additionally, the relative errors of the eigenfrequencies of the reduced assembly models obtained using both selection methods with respect to the unreduced assembly eigenfrequencies, are shown in Table 1.4. Here it is shown that, although all errors are negligibly small, the relative eigenfrequency errors obtained using the traditional method are smaller than those obtained using the proposed method for almost every eigenfrequency in the FROI. The discrepancy in relative eigenfrequency errors between both methods grows in the favor of the traditional method for increasing eigenfrequencies, which, although

Table 1.4 Eigenfrequencies of the unreduced assembly model and relative eigenfrequency errors of assembly models reduced using the proposed and traditional eigenmode-selection methods to retain 11 elastic free-interface substructure eigenmodes. Only the eigenfrequencies within the FROI are shown

Assembly eigenmode k	1	2	3	4	5	6	7	8
Eigenfrequency, unreduced [Hz]	0.0857058	0.685552	2.70482	6.39387	11.6312	17.0967	21.8219	29.9792
Relative error, proposed method [%]	1.27×10^{-6}	8.73×10^{-10}	-9.91×10^{-8}	-3.54×10^{-6}	-4.71×10^{-5}	-1.88×10^{-4}	-2.94×10^{-4}	-4.03×10^{-3}
Relative error, traditional method [%]	1.29×10^{-6}	1.31×10^{-9}	-3.25×10^{-8}	-8.26×10^{-7}	-5.05×10^{-6}	-4.40×10^{-6}	-1.06×10^{-4}	-3.39×10^{-4}

Table 1.5 Exact scalar assembly error measures obtained when the reduction is performed by selecting $n_{\mathcal{K}}^{(assy)}$ elastic free-interface substructure eigenmodes for HH reduction bases, using the traditional (cutoff frequency) and proposed (sensitivity-based) eigenmode-selection methods

$n_{\mathcal{K}}^{(assy)}$	$\chi^{(assy)}$ [−]	
	Traditional	Sensitivity-based
3	7.3343×10^{1}	5.7036×10^{0}
11	7.0686×10^{-3}	3.0286×10^{-3}
13	3.0401×10^{-3}	1.5924×10^{-3}

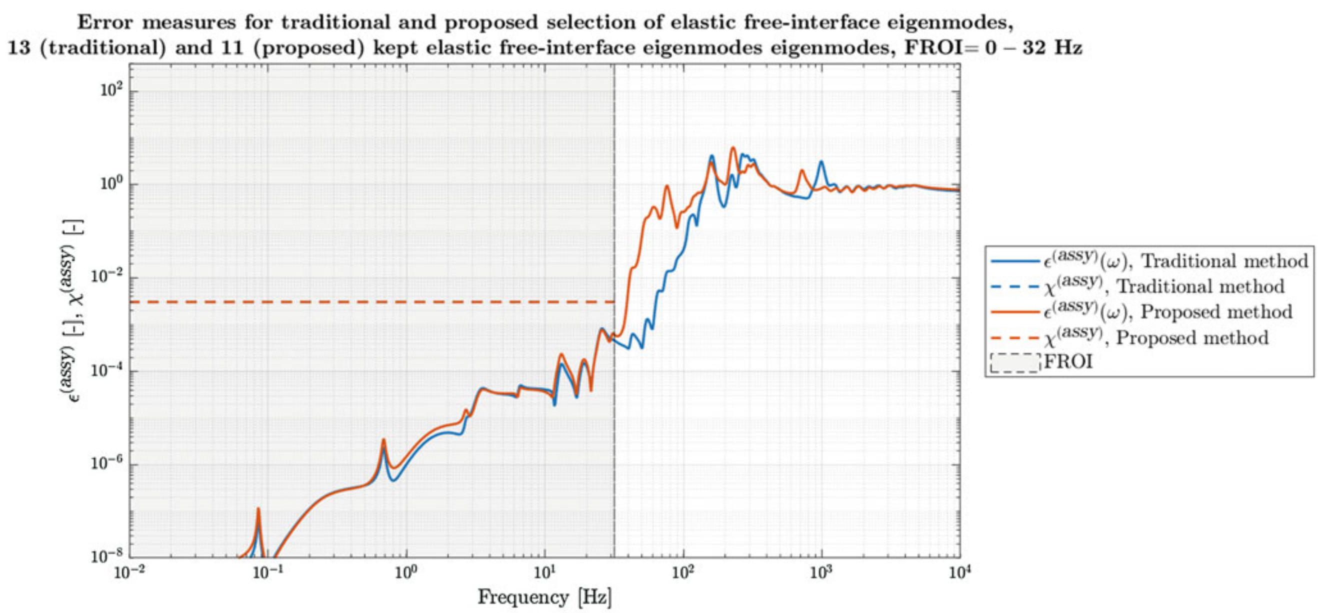

Fig. 1.6 Assembly receptance error measures $\epsilon^{(assy)}(\omega)$ and $\chi^{(assy)}$ obtained by using HH reduction bases where 13 elastic free-interface component eigenmodes are chosen using the traditional method and 11 using the proposed method. Note that the blue and red dashed lines practically coincide

not shown, can also be witnessed outside the FROI. This observation highlights that the proposed method focuses on approximating input–output behavior, but is also able to approximate eigenfrequencies with satisfactory accuracy.

The third use case shows how many eigenmodes should be selected using the traditional method such that the exact receptance error measure approximately equals the exact receptance error measure obtained using the sensitivity-based method in the second use case (where $n_{\mathcal{K}}^{(assy)} = 11$). As shown in Table 1.5, this is the case when 13 eigenmodes are selected using the traditional method. This situation is presented in Fig. 1.6, where the frequency-dependent error measures are comparable in the entire FROI. This use case thus shows that a smaller reduced model can be obtained with the proposed method, without increasing the reduction error compared to the traditional method.

1.5 Conclusions and Future Work

In this paper, a novel method for the selection of elastic free-interface substructure eigenmodes as used to reduce substructure models using the Hintz–Herting CMS method is proposed. The goal of this selection method is that the reduced assembly, obtained by coupling the reduced substructures, provides an accurate description of the frequency response functions at and between specific points of interest within a frequency range of interest. This goal is achieved by efficiently estimating assembly receptance reduction errors using sensitivities of the assembly receptance with respect to its substructure receptances and efficient descriptions of the substructure receptance error obtained using modal truncation error approximations. A leave-one-out approach is adopted to estimate the assembly receptance errors caused by the truncation of individual substructure eigenmodes. After condensing these estimated receptance errors using spatial and temporal norms, they are ranked by magnitude. The eigenmodes causing the highest approximate receptance errors are then selected for the set of kept eigenmodes as used in the substructure reduction bases. It has been shown that a selection of the eigenmodes obtained using the novel method results in accurately reduced assembly models. In fact, three use cases have been presented in which the sensitivity-based method outperforms the traditional selection method, which is solely based on cutoff frequencies. This observation highlights that the traditional method does not select an optimal set of retained eigenmodes. Therefore, using the sensitivity-based method for the selection of elastic free-interface eigenmodes, can provide the user with more accurate and/or efficient reduced assembly models than when the traditional selection method is used. Although, in this paper, the method has been applied to HH reduced substructure models, the method can be applied to other CMS methods using free-interface eigenmodes as well. Furthermore, it was explained that the selection of retained eigenmodes found by evaluating receptance errors is equivalent to evaluating mobility or inertance error matrices.

Despite the advantages shown here, it cannot be guaranteed that the proposed method will always outperform the traditional method, due to the approximative nature of the selection procedure. In fact, for some use cases based on the current demonstrator, the traditional method is found to perform (slightly) better. However, the used demonstrator is academic. For a (much) more complex engineering system such as a lithography machine, an airplane, or a ship, with more eigenmodes which act relatively locally, the sensitivity-based method is expected to only select local modes which are relatively important for specific assembly response behavior and truncate irrelevant (local) modes. It is expected that application of the sensitivity-based method to such more complex systems would show more clearly the benefit of the novel mode-selection method over the traditional selection method based on a cutoff frequency, certainly if the accuracy of only a limited number of FRFs (related to POIs) is important. This has to be investigated in the future. Furthermore, the novel selection method may be improved by adopting an iterative selection approach instead of the currently used leave-one-out approach. In such an iterative approach, the first eigenmode to be kept is selected as in the sensitivity-based method, but for each subsequently selected eigenmode it is taken into account that there is a set of eigenmodes already present in the reduced model. Although such an iterative method is computationally much more expensive, it might improve the reliability of the sensitivity-based method. Finally, instead of the first-order approximation of the assembly error used in this paper, higher-order approximations can be used. Even though this again comes at the cost of computation time, it could improve reliability of the proposed method as well.

References

1. Besselink, B., Tabak, U., Lutowska, A., Van De Wouw, N., Nijmeijer, H., Rixen, D.J., Hochstenbach, M.E., Schilders, W.H.: A comparison of model reduction techniques from structural dynamics, numerical mathematics and systems and control. J. Sound Vib. **332**(19), 4403–4422 (2013)
2. Craig, R.: Coupling of substructures for dynamic analyses – an overview. In: 41st Structures, Structural Dynamics, and Materials Conference and Exhibit (2000)
3. Craig, R., Bampton, M.: Coupling of substructures for dynamic analyses. AIAA J. **6**(7), 1313–1319 (1968)
4. De Klerk, D., Voormeeren, S.N.: Uncertainty propagation in experimental dynamic substructuring. In: Conference Proceedings of the Society for Experimental Mechanics Series, vol. 26 (2008)
5. De Klerk, D., Voormeeren, S.N.: Uncertainty propagation in experimental dynamic substructuring. Mech. Syst. Signal Proces. **24**, 106–118 (2010)
6. De Klerk, D., Rixen, D.J., De Jong, J.: The frequency based substructuring (FBS) method reformulated according to the dual domain decomposition method. In: Conference Proceedings of the Society for Experimental Mechanics Series, vol. 24 (2006)
7. de Kraker, B.: A Numerical-Experimental Approach in Structural Dynamics. Shaker Publishing, Maastricht (2004). ISBN 90-423-0259-3
8. Glover, K.: A tutorial on Hankel-norm approximation. In: From Data to Model, pp. 26–48 (1989)
9. Herting, D.N.: A general purpose, multi-stage, component modal synthesis method. Finite Elem. Anal. Des. **1**(2), 153–164 (1985)
10. Voormeeren, S.N.: Dynamic substructuring methodologies for integrated dynamic analysis of wind turbines. Ph.D. Thesis, Delft University of Technology (2012)